Published in final edited form as:
Lab Chip. 2011 March 21; 11(6): 1138–1143. doi:10.1039/c0lc00500b.

Hydrodynamic optical alignment for microflow cytometry†

Matthew J. Kennedy[a], **Scott J. Stelick**[b], **Lavanya G. Sayam**[c], **Andrew Yen**[c], **David Erickson**[d], and **Carl A. Batt**[b]

Carl A. Batt: cab10@cornell.edu

[a]Department of Electrical and Computer Engineering, Cornell University, Ithaca, NY, 14853, USA

[b]Department of Food Science, Cornell University, Ithaca, NY, 14853, USA

[c]Cornell Biomedical Sciences Flow Cytometry Core Laboratory, College of Veterinary Medicine, Cornell University, Ithaca, NY, 14853, USA

[d]Sibley School of Mechanical and Aerospace Engineering, Cornell University, Ithaca, NY, 14853, USA

Abstract

A microfabricated flow cytometer has been developed that is capable of detecting nearly all of the microparticles in an aqueous suspension. Current design allows for integrated coupling between an optical fiber-based detection system and the particle stream *via* hydrodynamic focusing. By adjusting the relative flow-rates at the auxiliary inputs of the focusing manifold, the particle stream can be steered out-of-plane relative to the illuminating laser, and similarly the particle stream can be squeezed or expanded. The microfabricated device was constructed in polydimethylsiloxane with cross-sectional microfluidic dimensions of 125 μm × 125 μm. Using the present device and method, fluorescent microparticles in aqueous solution were counted at an absolute counting efficiency of 91 ± 4%. The coefficient of variation of the fluorescence pulse-heights for far-red fluorescent microparticles was 15%. The device exhibited a linear response to fluorescence intensity calibration microparticles as shown by comparison with a commercial cytometer instrument.

Introduction

Conventional cytometers remain as large and immobile instruments requiring highly specialized personnel for operation and maintenance. Using microfabrication technology, it should be possible to manufacture inexpensive, portable cytometer devices operable by minimally trained personnel. Such portable technology is potentially useful for pathogen detection, environmental microbiology, and for the treatment of AIDS in rural parts of developing countries. Microfabricated cytometers have been demonstrated in research laboratory settings[1–3] but have not been manufactured on a large scale. Additional research and development is needed to demonstrate the feasibility and potential benefits of microfluidics for flow cytometry.

Micro-optics technologies are increasingly becoming integrated into microfluidic devices.[4,5] Imbedding the optics stabilizes the device to mechanical shock and reduces its overall space requirements. The coupling of optics with fluids remains an active area of research and continues to generate potentially useful technologies such as integrated lasers[6] and optical

†Electronic supplementary information (ESI) available: Details are provided regarding the measurement of the density of the stock solution of microparticles.

Correspondence to: Carl A. Batt, cab10@cornell.edu.

filters,[7] optofluidically adjustable lenses[8] and waveguides,[9] and MEMS-based mirror arrays.[10] Preliminary microflow cytometers have been demonstrated using one or more of these emerging technologies.[5,11] In recent work, Rosenauer *et al.* used a micro-fabricated cylindrical lens in combination with a microfabricated multimode waveguide to deliver an illuminating beam of only 15 μm width at the center of the microfluidic channel.[5] However the majority of microflow cytometers have used either free-space optics[12,13] or imbedded optical fibers.[4,14,15] While new micro-optics technologies continue to undergo development, at this time imbedded optical fibers provide a convenient approach for exploring the potential benefits of integrating micro-optics into microfluidic devices.

Three-dimensional focusing devices focus a suspension into a cylindrical lamina positioned near the center of the micro-channel.‡ Three-dimensional focusing has been accomplished hydrodynamically using bas-relief structures,[16] inertial vortices,[12,17] and multi-layer manifolds.[18,19] An advantage of the multi-layer manifolds is their capability of out-of-plane steering of the focused stream.[19]

Golden *et al.* developed a microflow cytometer inclusive of three-dimensional hydrodynamic focusing and an optical fiber-based detection system.[16] The present device follows the general architecture of Golden *et al.* but provides the additional capability of out-of-plane steering of the particle stream. Other devices have been reported containing this capability in their architecture,[3,5] however the present study is the first to acquire data with the particle stream positioned at different locations and the first to measure absolute counting efficiency.

Development of a microflow cytometer requires an understanding of how device design affects the optical signal. The coefficient of variation (CV) of fluorescent pulses provides an indicator of optical signal quality for a flow cytometer. Minimizing the CV is important for achieving maximum detection sensitivity and for achieving maximum multiplexing capability. In the present study, the signals generated using our micro-fabricated flow cytometer are compared with those generated using a large-scale commercial instrument.

Methods

Device

The device comprised a hydrodynamic focusing manifold and imbedded optical fibers, as illustrated in Fig. 1. The hydrodynamic focusing manifold was described in detail in our previous work[19] and consisted of a two-layer structure in which the particle stream was impinged first from below and then from above by focusing fluids from the adjoining layer. The particle stream was injected at volumetric flow-rate U_1, and the upper and lower focusing fluids were injected at rates U_2 and U_3, respectively. The three independent flow-rates, U_1, U_2, and U_3, were driven by three syringe pumps (PHD 2000, Harvard Instruments). In the present study, the total volumetric flow-rate was fixed at $U_{TOT} = 55\ \mu L\ min^{-1}$, corresponding to an average fluid velocity of $u_{AVG} = 5.9\ cm\ s^{-1}$. The focusing fluids were added from both sides such that the total volumetric flow-rate was $U_{TOT} = U_1 + 2U_2 + 2U_3$.

The focused stream can be squeezed or expanded *via* the focusing ratio, defined as the fractional volumetric flow-rate of focusing fluids, $U_{FOCUS}/U_{TOT} = (2U_2 + 2U_3)/U_{TOT}$. Multi-physics simulations show the focused stream at three focusing ratios in Fig. 2. These simulations followed the concentration distribution of indicator dye with a diffusion

‡Strictly speaking, this type of focusing acts in only two dimensions, however in practice the microfluidics community has referred this as three-dimensional focusing.

coefficient of 1×10^{-10} m^2 s^{-1}. Noticeably, some diffusion of the indicator occurred in the hydrodynamic focusing region resulting in lower absolute concentrations at higher focusing ratios. The multiphysics simulation procedures were explained in detail and were verified by confocal microscopy in our previous work.[19] The height and width of the focused stream were measured using ImageJ according to the full-width-at-half-max.

The device was fabricated at the Cornell NanoScale Science and Technology Facility according to the methods described in detail in our previous work.[19] The feature height of the micro-fluidic channels was 125 μm, which corresponds to the diameter of a standard optical fiber. Briefly, two complementary pieces of polydimethylsiloxane (PDMS) microfluidics housing were replica-molded from their respective masters. The masters were fabricated on silicon wafers by photolithographic patterning of polyimide resist (SU-8, Microchem). Prior to pouring the PDMS onto the silicon masters, a hydrophobic coating was applied to the silicon masters by spin-coating of RAIN-X followed by rinsing with isopropyl alcohol. During molding, the PDMS was spun onto the masters at 160 revolutions per minute for 40 seconds in order to form molds of uniform thickness. Achieving uniform thickness was important for achieving good alignment between the two pieces, to within 10 μm or better, during the contact alignment step. The PDMS was cured by baking at 70 °C for 100 minutes. The pieces of PDMS were peeled from their respective masters, exposed to a 200 W oxygen plasma for 20 s, and brought into contact using a contact aligner. Then, the PDMS was baked post-contact alignment for an additional 15 min at 70 °C to promote permanent adhesion. Tubing was inserted into lithographically defined tubing inputs. The PDMS–tubing structure was placed on a glass microslide for structural support, and the tubing–PDMS interface was sealed with epoxy (Hysol E-60HP, LocTite, USA). After the epoxy had cured, optical fibers were inserted into lithographically defined fiber insertion guides and fixed into place using optical adhesive (Norland Optical Adhesive #63).

Materials and reagents

The focusing solution consisted of 1 mM EDTA, 2 mM potassium phosphate monobasic, 16.6 mM sodium phosphate dibasic, 3.8 mM potassium chloride, and 139 mM sodium chloride, adjusted to pH 7.4, with 0.05% Tween-20. The focusing solution was stored at 7× concentration without surfactant to inhibit contamination by yeast. Immediately prior to experiment, the focusing solution was diluted to its final concentration, then syringe-filtered using a 0.2 μm syringe filter in order to remove particulates, and finally autoclaved for 15 minutes and cooled in the refrigerator in order to remove trapped gases thereby mitigating the formation of bubbles inside the microfluidic device. The particle suspension buffer consisted of focusing solution with 30% polyethylene glycol added, molecular weight 3350 g mol^{-1}. The purpose of adding the polyethylene glycol was to match the density of the solution to that of the particles thereby preventing the particles from settling out of solution onto the bottom of the syringe barrel at run-time. The particle suspension buffer was syringe-filtered proceeding addition of polyethylene glycol and preceding addition of microparticles. The device was operated in the horizontal configuration.

Intensity calibration particles specific for 633 nm excitation and 660 nm emission were purchased from Invitrogen (Linear-Flow™ Deep Red Flow Cytometry Intensity Calibration Kit). This kit contained six particle-sets packaged in individual containers at an approximately common concentration. These particles were 6 μm in diameter. Only the brightest set of particles from the kit was used for measuring the absolute counting efficiency of the micro-flow cytometer. The particle-density for this particular set of particles was measured at the Cornell Core Flow Cytometry Facility on a commercial flow cytometer instrument (LSR II, Becton Dickinson) using a co-suspension of absolute counting microparticles (CountBright™, Invitrogen), and the measured particle concentration was $1.54 \pm 0.06 \times 10^7$ mL^{-1} (see ESI†). These brightly fluorescent particles

were used for measuring absolute counting efficiency because they were easily distinguishable from spurious noise. Notably, CountBright™ bsolute counting particles were available, however distinguishing these particles from spurious events was difficult using the microfluidic device due to their low fluorescence signal and also because only large angle scatter was available for this micro-fluidic device as opposed to the combination of forward scatter and side scatter typically found in the commercial instruments. A 50× dilution of these particles was used for characterizing the microfabricated device in order to limit reagent consumption.

Optical detection system

A bright-field micrograph shows the optical interrogation zone in Fig. 3. A 5 mW 633 nm HeNe Laser was used as an excitation source and was delivered at an angle of 90° with the microfluidic channel. Three signals were acquired simultaneously using three identical photomultiplier tubes (PMTs) (H5784, Hamamatsu, Japan): side-scatter at 45° (SS 45), side-scatter at 135° (SS 135), and fluorescence at 660/30 (660/30). A single-mode fiber with a cutoff wavelength of 500–600 nm was used for laser delivery (F-SV, Newport). Multimode fibers were used for photon collection.

Electronic power supplies were constructed which supplied source voltages to the PMTs using DC–DC converters (DKE10A-15, Mean-well, USA). The control voltages, *i.e.* gains, applied to the PMTs were tuned between 0 V and 1 V using potentiometer-based resistive voltage dividers and were monitored using panel LCD voltage monitors (DMS-20LCD-1-5-C, Murata Power Solutions).

Data were acquired by recording signals from the PMTs using a multi-channel digital oscilloscope (WaveRunner 6050, LeC-roy). The entrance of each PMT was fixed to a collimation tube containing optical filters and an optical fiber adapter. The entrance to the fluorescence detector was filtered using a 660/30 bandpass filter and a 632 nm notch filter (Chroma, USA), and the scattering detectors were filtered using 632/10 bandpass filters (Thorlabs). Note that six fibers were imbedded in the device, but only four of these were used in the present study. Therefore, it would be straightforward to add an additional laser and photodetector for quantifying fluorescein-labeled target for the analysis of a multiplexed particle-based assay, as demonstrated previously by Kim *et al.*[2]

The optical detection zone can be visualized by examining the distribution of the pulse-durations. Specifically, the mean pulse-duration was 0.54 ± 0.08 ms for SS 45 pulses. Assuming the particles were traveling at the mean fluid velocity, $u_{AVG} = 5.9$ cm s^{-1}, the beam waist was 32 ± 5 μm. [§] This length agrees approximately with the streak-length of the particle through the optical beam. The mode field was 5 μm in diameter inside the optical fiber. Since the tip of the fiber was located 100 μm from the center of the microfluidic channel, the suggested angle of divergence of the laser out of the tip of the fiber was approximately 10°.

Data acquisition and processing

Oscilloscope traces were acquired and saved as individual binary oscilloscope files onto an external hard disk drive. Waveform collection was triggered on SS 45 using AC coupling, and SS 135 and 660/30 were acquired using DC coupling. After data collection was

[†]Electronic supplementary information (ESI) available: Details are provided regarding the measurement of the density of the stock solution of microparticles.

[§]In the field of optics, the beam waist is commonly described according to its full-width at half-max, which was smaller, by a factor of approximately 2, in comparison to the measurement used here, which was based on the threshold-crossing points at four standard deviations above baseline.

complete, the waveforms were digitally processed using a MATLAB script. This script first low-pass-filtered all three signals using a time-domain mean filter with an integration time of 5 μs. Then, the script thresholded the SS 45 signal at four standard deviations above baseline. A large number of waveforms were processed and parameterized in terms of pulse-duration, pulse-height, and pulse-area. The pulse duration was determined by the threshold-crossing times. The pulse-area was determined by the integral of the voltage signal over the pulse duration. The pulse-height was determined by the local maximum of the low-pass-filtered signal.

Two experiments were performed in the present work requiring different data acquisition protocols: absolute counting efficiency was measured as the particle stream was maneuvered up and down relative to the illuminating beam, and the CV of the fluorescence pulse-heights was determined for the microfluidic device and for a large-scale commercial instrument.

For measuring absolute counting efficiency, the particle suspension was positioned first at the bottom of the micro-channel and then translated upward in steps to the top of the microchannel. At each step in U_3/U_2, more than 150 waveforms were collected each of 500 ms duration. The triggering threshold on the oscilloscope was set sufficiently low to trigger the waveforms on random noise in the SS 45 channel. A typical photon-burst was less than 1 ms in duration, and a typical waveform contained several photon-bursts. The gain for the SS 45 photo-detector was maintained sufficiently high to reach saturation during the passage of a particle; the gains for the other photo-detectors were not saturated. Spurious events were triggered on SS 45, but these did not affect the final particle count, which was determined by gating on SS 135 and 660/30.

For measuring the CV of the fluorescence pulse-heights, a mixture containing six sets of particles from the LinearFlow™ intensity standard calibration kit was analyzed under the condition of $U_3/U_2 = 1.0$ and $U_{FOCUS}/U_{TOT} = 0.90$. Waveforms of 5 ms duration were triggered on SS 45 and collected at a 200 MHz rate of digitization. A total of 1000 sets of waveforms were collected. Typical pulses were about 1 ms in duration, and a typical waveform contained only one photon-burst event. Events were gated on SS 135 *vs.* SS 45 in order to eliminate spurious events.

Results and discussion

Hydrodynamic alignment of the particle stream with the optical detection system

The particle stream was maneuvered up and down within the microchannel by sweeping the ratio between the upper and lower focusing fluids, U_3/U_2. The step-size in U_3/U_2 corresponded to out-of-plane displacement of the focused stream by 8 μm. Three different focusing ratios were used with higher focusing ratios corresponding to tighter focusing of the particle stream. The number of gated events was compared with the known rate of particle throughput yielding absolute counting efficiency. In this way, absolute counting efficiency was measured as a function of U_3/U_2, as shown in Fig. 4. The events were gated in MATLAB from a scatter-plot of 660/30 *vs.* SS 135 in order to eliminate spurious events not corresponding to particles. A single 3 mL particle suspension was used to acquire all of the data points shown in Fig. 4 during continuous operation on one day.

The maximum absolute counting efficiency measured was 91 ± 4%, which was observed at a focusing ratio of $U_{FOCUS}/U_{TOT} = 0.99$ (Fig. 4). Many of several competing effects may explain why the measured absolute counting efficiency was less than 100%: stray beads may pass undetected, and beads may stick to the surfaces of the syringe barrels, needles, tubing, and microchannels. It might be possible to increase the measured maximum absolute counting efficiency slightly beyond 91 ± 4% by using a finer step-size in U_3/U_2. However,

the increase would likely be subtle considering the small displacement of the particle stream relative to the stream height and also considering the measurement uncertainty.

A trade-off existed between absolute counting efficiency and particle throughput, as shown in Table 1. At high throughput, *i.e.* $U_{FOCUS}/U_{TOT} = 0.90$, the maximum absolute counting effi-ciency was only 58 ± 4%. If desired, greater particle throughput can be achieved by increasing the total volumetric flow-rate. For example, a similar device was operated successfully by Kumm-row *et al.* at a total volumetric flow-rate of up to 1 mL min^{-1},[3] nearly 20× greater than that used in the present study.

The illumination-guiding optical fiber was not aligned with the vertical center of the microchannel as intended. Rather, the data in Fig. 4 indicate that, upon comparison with multiphysics simulations,[19] at maximum detection efficiency the vertical position of the particle stream was located at $y_{CM} = 0.63$, *i.e.* displaced vertically upwards from center by 13% of the micro-channel height, or 16 μm. This misalignment is a fabrication issue and can be resolved in future devices. Importantly, hydrodynamic optical alignment provides a run-time work-around for device-to-device inconsistencies arising from the fabrication process.

Multiplexed detection of microparticles of varying fluorescence intensity

Intensity calibration particles with six relative median fluorescence intensities (MFIs) ranging from 0.05% to 100% were combined into a mixture and analyzed using the microflow cytometer. Due to the intensity profile of the illuminating beam, particles passing through the center of the optical beam scattered more light and also emitted more fluorescence than particles passing through the edge of the beam. This effect was corrected mathematically using a simple mathematical normalization procedure described previously by Golden *et al.*[16] Scatter plots show the effect of this normalization procedure on the data in Fig. 5. Most events from the faintest two populations occurred within the noise floor of the signal, and during the normalization procedure many of these events were transformed into the gate for the fourth population. Given access to improved data acquisition electronics, all six particles should be simultaneously detectable using the present device. The limitation of detecting only four out of six beads arose from the 8-bit analog-to-digital converter present in the oscilloscope available for our use resulting in less than two-and-a-half logs of digitization, *i.e.* values ranging between zero and 255. Meanwhile, the commercial instrument used a 16-bit analog-to-digital converter resulting in more than four-and-a-half logs of digitization, *i.e.* values ranging between zero and 65 535. For sizing applications, it may be useful to normalize the SS 135 signal by a second scattering signal, such as SS 45.

Identical mixtures of intensity calibration microparticles were analyzed using the microfabricated device and using the commercial instrument, and the two sets of results are compared in Fig. 6. Both sets of data were fit analytically by assuming a normal distribution about their MFIs using a digital fitting procedure in MATLAB. The values for MFI, CV, and the number of events are listed in Table 2 for both of these analyses. Both the microflow cytometer and the commercial instrument used 633 nm lasers and 660 nm centered bandpass fluorescence filters. The microflow cytometer exhibited a characteristic CV of 15% whereas the large-scale commercial instrument exhibited a characteristic CV of 6%.

The commercial instrument exhibited superior signal quality compared with the microfabricated device as indicated by their CVs. Two likely sources exist for the change in signal quality on moving to the microfabricated device: the optical fibers and the microfluidic channel. Optical fibers possess fundamental limitations such as limited numerical aperture. The microfluidic channel might distribute the fluids over a wider range of velocities than the flow-cell in a large-scale commercial instrument.

To date, the optical-fiber-based devices have not matched the CV of their free-space-optics-based counterparts. In one study, Kummrow *et al.* analyzed a microfluidic device using both optical fibers and free-space optics, and while CV measurements were reported only for the free-space optics, the authors mentioned that the pulse-height distributions were slightly narrower using free-space-optics compared with optical fibers.[3] In another study, Simonnet and Groisman achieved CVs in the range of 3–6%, rivaling the performance of the commercial instruments, by using an objective lens with a high numerical aperture (63×/1.25).[20] Our results agree well with the previous study by Golden *et al.*, which used a similar optical fiber-based detection system and which reported a similar CV of 15%. Altogether, the available literature suggests that the optical fibers are primarily responsible for the decrease in the signal quality of the microfabricated device compared with the large-scale commercial instrument, however hydrodynamics also may have contributed significantly to the decrease in signal quality. Specifically, in order to accommodate the fabrication-misaligned optical fibers, the particle stream was displaced upwards from the center of the microchannel into a region of wider ranging fluid velocity. In addition, the CV was measured using focusing ratio $U_{FOCUS}/U_{TOT} = 0.90$, which distributed the focused stream over a large region of the microchannel compared with higher focusing ratios. Therefore, signal quality in the present device might be improved by squeezing the core flow into a smaller stream and by positioning the stream in a region of minimal velocity variation.

The microflow cytometer exhibited a linear response to fluo-rescence intensity as verified by comparing the MFIs measured using the microflow cytometer with those measured using the commercial instrument, as shown in Fig. 7. For the three brightest particle sets, the root-mean-squared-relative-error from linear fit was less than 0.1% whereas for the fourth-brightest particle set the relative error was 7% due to the limited resolution, at 8 bits, of the analog-to-digital converter present in the oscilloscope.

Conclusions

A microflow cytometer has been developed in which the optical alignment between the particle stream and the laser is optimized hydrodynamically. The method of hydrodynamic optical alignment provides an automatable method for aligning micro-fabricated cytometer-based devices with an accepting instrument at run-time. The device and method make it possible to detect nearly all of the particles present in the suspension. This capability reduces the quantity of reagents necessary to perform a particle-based assay thereby reducing the cost per analysis for such a device.

A variety of microfluidic geometries and optical elements are available for integration into microflow cytometers. For sample injection, three-dimensional focusing has become preferred over two-dimensional focusing,[2,3,12,16,20] however for illumination and photon collection, it remains unclear whether micro-optics will become preferred over free-space optics. To date micro-optics-based cytometers have not matched their free-space-optics-based counterparts with regard to signal quality. Still, further development of micro-optics-based cytometers is justified. Substantial improvements in signal quality may be achievable by improved alignment of the imbedded optics relative to the geometric center of the microchannel, further development of micro-optical beam-shaping elements, and minimization of hydrodynamic variation of the velocities of the particles. At this time, microflow cytometry remains in search of an imbedded architecture for delivering laser power to the geometric center of a microchannel.

Supplementary Material

Refer to Web version on PubMed Central for supplementary material.

Acknowledgments

The micro-flow cytometer was fabricated at the Cornell Nano-Scale Science and Technology Center, a member of the National Nanotechnology Infrastructure Network, which is supported by the National Science Foundation. Analysis using the commercial LSR II cytometer was performed at the Cornell Biomedical Sciences Flow Cytometry Core Laboratory. A.Y. is grateful to United States Public Health Service (National Institute of Health) and New York State Stem Cell Science (NYSTEM) for support. M.J.K. thanks Clifford R. Pollock for useful conversations on waveguides and optical modes.

References

1. Yang SY, Lien KY, Huang KJ, Lei HY, Lee GB. Biosens Bioelectron. 2008; 24:855–862. [PubMed: 18760591]
2. Kim JS, Anderson GP, Erickson JS, Golden JP, Nasir M, Ligler FS. Anal Chem. 2009; 81:5426–5432. [PubMed: 19496600]
3. Kummrow A, Theisen J, Frankowski M, Tuchscheerer A, Yildirim H, Brattke K, Schmidt M, Neukammer J. Lab Chip. 2009; 9:972–981. [PubMed: 19294310]
4. Wang Z, El-Ali J, Perch-Nielsen IR, Mogensen KB, Snakenborg D, Kutter JP, Wolff A. Lab Chip. 2004; 4:372–377. [PubMed: 15269807]
5. Rosenauer M, Buchegger W, Finoulst I, Verhaert P, Vellekoop M. Microfluid Nanofluid. 10.1007/s10404-010-0707-z
6. Li Z, Zhang Z, Emery T, Scherer A, Psaltis D. Opt Express. 2006; 14:696–701. [PubMed: 19503387]
7. Llobera A, Demming S, Joensson HN, Vila-Planas J, Andersson-Svahn H, Buttgenbach S. Lab Chip. 2010; 10:1987–1992. [PubMed: 20485776]
8. Rosenauer M, Vellekoop MJ. Lab Chip. 2009; 9:1040–1042. [PubMed: 19350083]
9. Wolfe DB, Conroy RS, Garstecki P, Mayers BT, Fischbach MA, Paul KE, Prentiss M, Whitesides GM. Proc Natl Acad Sci U S A. 2004; 101:12434–12438. [PubMed: 15314232]
10. Chiou PY, Ohta AT, Wu MC. Nature. 2005; 436:370–372. [PubMed: 16034413]
11. Yin D, Lunt EJ, Rudenko MI, Deamer DW, Hawkins AR, Schmidt H. Lab Chip. 2007; 7:1171–1175. [PubMed: 17713616]
12. Mao X, Lin SC, Dong C, Huang TJ. Lab Chip. 2009; 9:1583–1589. [PubMed: 19458866]
13. McClain MA, Culbertson CT, Jacobson SC, Ramsey JM. Anal Chem. 2001; 73:5334–5338. [PubMed: 11721938]
14. Fu LM, Yang RJ, Lin CH, Pan YJ, Lee GB. Anal Chim Acta. 2004; 507:163–169.
15. Tung YC, Zhang M, Lin CT, Kurabayashi K, Skerlos SJ. Sens Actuators, B. 2004; 98:356–367.
16. Golden JP, Kim JS, Erickson JS, Hilliard LR, Howell PB, Anderson GP, Nasir M, Ligler FS. Lab Chip. 2009; 9:1942–1950. [PubMed: 19532970]
17. Bhagat AAS, Kuntaegowdanahalli SS, Necati K, Seliskar CJ, Papautsky I. Biomed Microdevices. 2010; 12:187–195. [PubMed: 19946752]
18. Chang CC, Huang ZX, Yang RJ. J Micromech Microeng. 2007; 17:1479–1486.
19. Kennedy MJ, Stelick SJ, Perkins SL, Cao L, Batt CA. Microfluid Nanofluid. 2009; 7:569–578.
20. Simonnet C, Groisman A. Anal Chem. 2006; 78:5653–5663. [PubMed: 16906708]

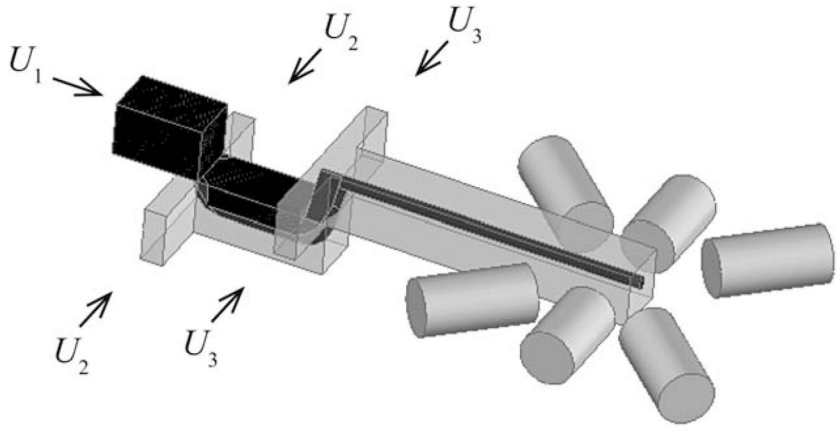

Fig. 1.

Schematic of the microflow cytometer. Illustration shows the hydrodynamic focusing manifold leading into an optical fiber-based illumination zone. The particle suspension was injected at volumetric flow-rate U_1, and the lower and upper focusing fluids were injected at rates U_2 and U_3, respectively.

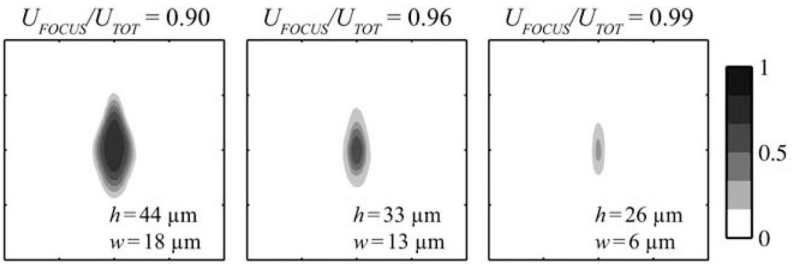

Fig. 2.

Contour plots show the focused stream according to multiphysics simulations for three different focusing ratios. The height, *h*, and width, *w*, of the focused stream are indicated according to its full-width-at-half-max. The microchannel was 125 μm wide and 125 μm tall. The tickmarks are separated by 31.25 μm. The contour scale indicates the concentration of indicator dye.

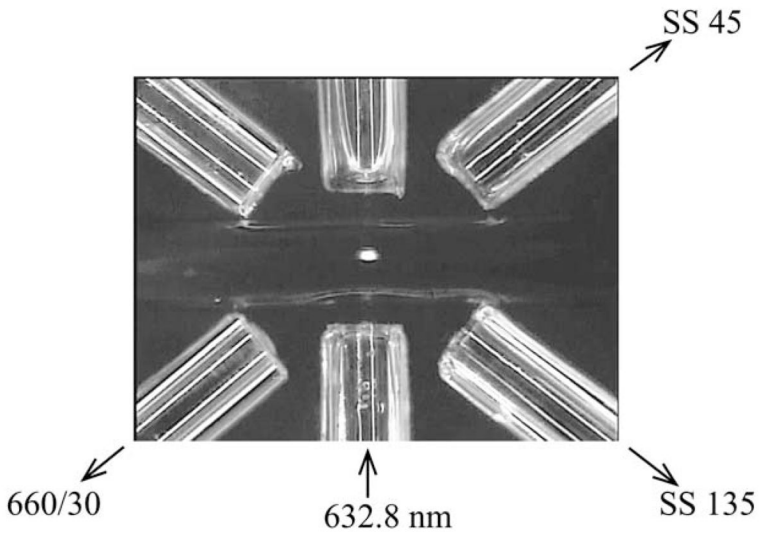

Fig. 3.

Brightfield micrograph shows the optical interrogation zone of the microflow cytometer. The width of the microchannel and the diameter of the optical fibers were both 125 μm. Using optical fibers, scattered radiation was collected at angles of 45° and 135°, and fluorescence was collected at 660 nm with a bandwidth of 30 nm. A fluorescence intensity calibration particle, 6 μm in diameter, is shown passing through the illuminating beam. The mean fluid velocity was 5.9 cm s^{-1}.

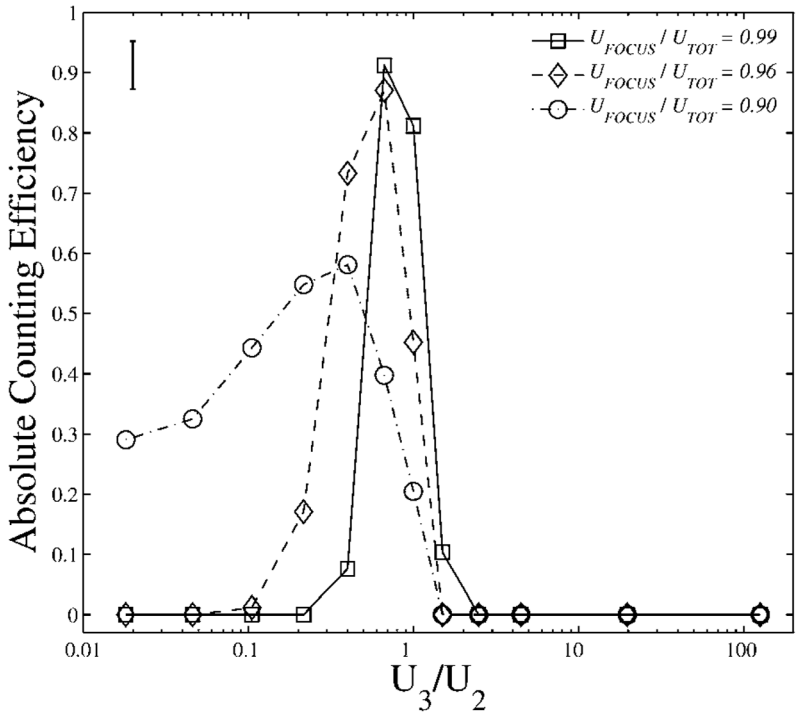

Fig. 4.

Plot shows the absolute counting efficiency of far-red fluorescent microparticles as a function of the ratio between the upper and lower focusing fluids, U_3/U_2, for data acquired at three focusing ratios, U_{FOCUS}/U_{TOT}. The relative error between measurements was approximately equal to the marker size. The absolute error is represented by the error bar at upper left, which reflects the uncertainty associated with the particle density in the stock particle solution. The step-size between successive data points along the horizontal axis corresponds to an 8-μm out-of-plane displacement of the focused stream.

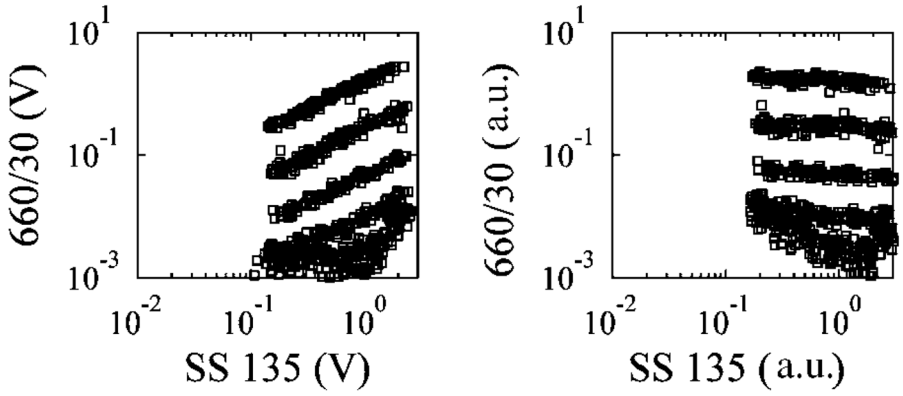

Fig. 5.
Scatter plots show the effect of the digital normalization procedure in which the fluorescence pulse-heights were normalized by the scattering pulse-heights. The raw pulse-heights were in units of volts (V), and the normalized pulse-heights were in arbitrary units (a.u.).

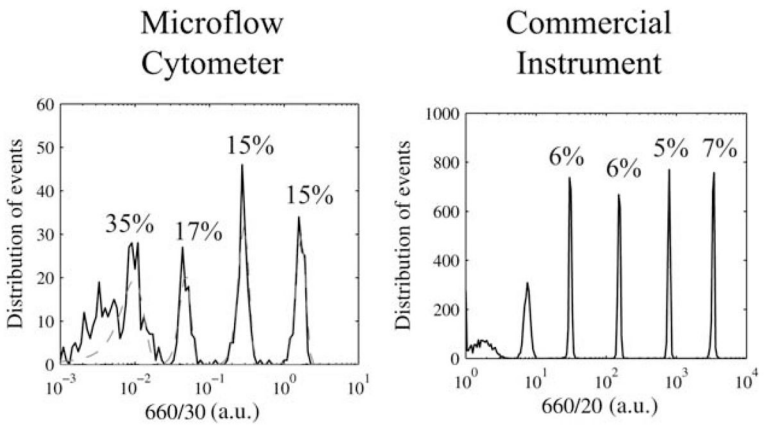

Fig. 6.

Histograms show the fluorescence pulse-height distributions for a mixture of LinearFlow™ fluorescence intensity calibration microparticles analyzed using the microfluidic device (left) and using the commercial instrument (right). Dashed curves show analytical fits according to the normal distribution. The left histogram shows a total of 600 gated events, and the right histogram shows a total of 10 000 gated events.

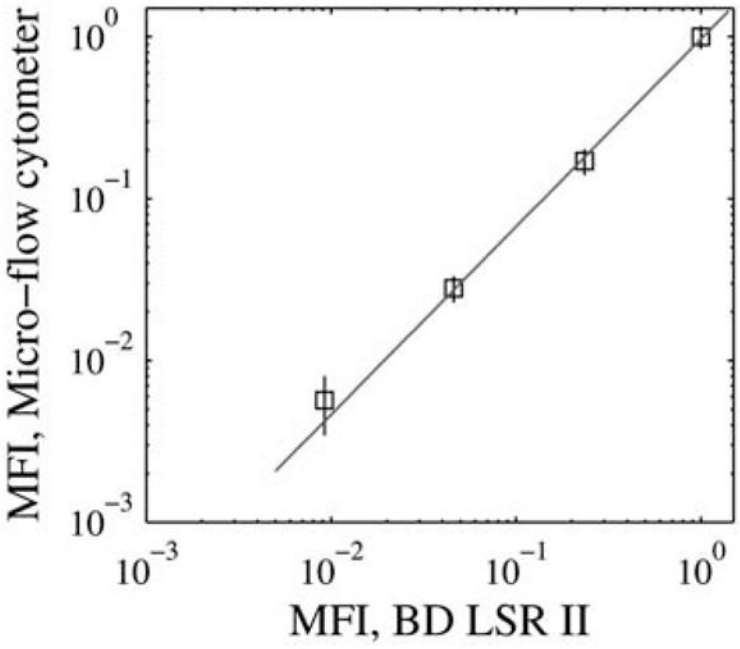

Fig. 7.

Plot shows the MFIs obtained for each of the four brightest particles in the LinearFlow™ fluorescence intensity calibration kit as measured using the microfluidic device and also using the commercial instrument. A linear model was fit through the brightest three particle-sets and extended down to the fourth particle-set.

Table 1

Maximum absolute counting efficiency measured for each of three focusing ratios

Focusing ratio	**0.90**	**0.96**	**0.99**
Sample throughput/μL min^{-1}	5.5	2.0	0.75
Max. abs. counting efficiency	58 ± 4%	87 ± 4%	91 ± 4%

Table 2

MFI, CV, and the number of gated events (*N*) for the brightest four subsets of particles from the LinearFlow™ fluorescence intensity calibration kit, as measured using the microflow cytometer and as measured using the large-scale commercial instrument.[a] The MFIs for the two datasets were normalized by the values corresponding to the brightest subset of particles

	Particle 1	Particle 2	Particle 3	Particle 4
Micro-flow cytometer				
MFI	1.00	0.17	0.028	0.0057
CV	15%	15%	17%	35%
N	123	149	98	215
Commercial instrument				
MFI	1.00	0.24	0.046	0.0092
CV	7%	6%	6%	6%
N	1717	1633	1643	1797

[a] LSR II, Becton Dickinson and Company.